Weighted linear least squares estimation of diffusion MRI parameters: strengths, limitations, and pitfalls

Jelle Veraart*[,a], Jan Sijbers[a], Alexander Leemans[b], Stefan Sunaert[c], Ben Jeurissen[a]

[a] *iMinds Vision Lab (Dept. of Physics), University of Antwerp, Antwerp, Belgium*
[b] *Image Sciences Institute, University Medical Center Utrecht, Utrecht, The Netherlands*
[c] *Department of Radiology, Faculty of Medicine, KU Leuven, Leuven, Belgium*

Abstract

Purpose: Linear least squares estimators are widely used in diffusion MRI for the estimation of diffusion parameters. Although adding proper weights is necessary to increase the precision of these linear estimators, there is no consensus on how to practically define them. In this study, the impact of the commonly used weighting strategies on the accuracy and precision of linear diffusion parameter estimators is evaluated and compared with the nonlinear least squares estimation approach. **Methods:** Simulation and real data experiments were done to study the performance of the weighted linear least squares estimators with weights defined by (a) the squares of the respective noisy diffusion-weighted signals; and (b) the squares of the predicted signals, which are reconstructed from a previous estimate of the diffusion model parameters. **Results:** The negative effect of weighting strategy (a) on the accuracy of the estimator was surprisingly high. Multi-step weighting strategies yield better performance, in some cases, even compared to the nonlinear least squares estimator. **Conclusion:** If proper weighting strategies are applied, the weighted linear least squares approach shows high performance characteristics in terms of accuracy/precision and may even be preferred over nonlinear estimation methods.

Key words: DTI, DKI, least squares, accuracy, precision, weight matrix, parameter estimation, diffusion, MRI

---

1. Introduction

Diffusion magnetic resonance imaging (dMRI) is currently the only method for the in vivo and non-invasive quantification of water diffusion in biological tissue (Bihan and Johansen-Berg, 2012). Several diffusion models have been proposed to obtain quantitative diffusion measures, which could provide novel information on the structural and organizational features of biological tissues, the brain white matter (WM) in particular. Typical examples of such diffusion models are diffusion tensor imaging (DTI; (Basser et al., 1994b)) and diffusion kurtosis imaging (DKI; (Jensen et al.,

*Corresponding author:
Jelle Veraart
iMinds Vision Lab, Dept. of Physics
University of Antwerp
Universiteitsplein 1, N 1.16
2610 Wilrijk, Belgium
Jelle.Veraart@ua.ac.be
+32 (0) 3 265 24 58
+32 (0) 3 265 22 45

2005)). Both diffusion models have in common that they can be linearized by the natural log-transformation for computing the model parameters. Despite the overwhelming literature on *advanced* diffusion (kurtosis) tensor estimation (e.g., Andersson, 2008; Kristoffersen, 2007, 2011; Jones and Basser, 2004; Koay et al., 2009; Veraart et al., 2011, 2012; Landman et al., 2007), the class of linear least squares (LLS) estimators is still widely used in diffusion MRI due to its low computational cost and ease of use.

It is well recognized that the variance of a log-transformed diffusion-weighted (DW) signal depend on the signal itself (Basser et al., 1994a; Koay et al., 2006; Salvador et al., 2005). A set of log-transformed DW signals, which is often used to linearly estimate the diffusion model parameters, is thus heteroscedastic. Therefore, a weighted linear least squares (WLLS) approach with well-defined weights, i.e. the inverse of the log-transformed signals' variances, is expected to provide more precise diffusion parameter estimates, at least, compared to its unweighted linear alternative. Optimal performance of the linear estimators can thus only be achieved if the variance of the log-transformed MR signals is known. Salvador et al. (2005) showed that this variance is a function of the unknown noise-free signal if the magnitude MR data is Rician distributed. Obviously, the noise-free signals are not known and, as such, the weight terms need to be estimated. Different ways to approximate the theoretically optimal weights have been suggested (Basser et al., 1994b; Salvador et al., 2005) and adopted by the community. A consensus on how the use the WLLS in practice has thus not been reached yet. Most often, information on the weighting is even not provided in scientific reports or software documentation. In this study, we will evaluate the impact of the different weighting strategies on the performance of the linear diffusion parameter estimators. Additionally, we will compare the linear estimators to their nonlinear alternative (Koay et al., 2006) in terms of accuracy and precision. By doing so, we aim to obtain more insight in the strengths, limitations, and potential pitfalls of the simple, though elegant, class of linear estimators.

2. Materials and methods

2.1. Diffusion models

The natural logarithm of the DW MR signal, S, can be expanded in powers of the wave number q in a zero-centered neighborhood (Kiselev, 2010). This expansion is known as the cumulant expansion, with DTI and DKI being the three-dimensional generalization of the second and fourth order cumulant expansion, respectively (Basser et al., 1994b; Lu et al., 2006). Both models are generally expressed in terms of the diffusion sensitizing gradient strength (b) and its direction ($\boldsymbol{g}$):

$$\begin{aligned}\ln S(b, \boldsymbol{g}) = \ln S(0) - b \sum_{i,j=1}^{3} g_i g_j D_{ij} \\ + \frac{b^2}{6}\left(\sum_{i=1}^{3}\frac{D_{ii}}{3}\right)^2 \sum_{i,j,k,l=1}^{3} g_i g_j g_k g_l W_{ijkl}.\end{aligned} \qquad [1]$$

In Eq. [1], $S(0)$ is the non-DW signal, $\boldsymbol{D} = \{D_{i,j} : i, j = 1, ..., 3\}$ the (apparent) diffusion tensor, and $\boldsymbol{W} = \{W_{ijkl} : i, j, k, l = 1, ..., 3\}$ the (apparent) kurtosis tensor. Because both tensors are fully symmetric, $\boldsymbol{D}$ and $\boldsymbol{W}$ have 6 and 15 degrees of freedom, respectively.

2.2. Tensor estimation

Consider a set of independently Rician distributed DW images $\tilde{\boldsymbol{S}} = \{\tilde{S}(b_i, \boldsymbol{g}_i) : i = 1, ..., N\}$. The natural logarithm of $\tilde{\boldsymbol{S}}$ can be modeled as (Basser et al., 1994b):

$$\boldsymbol{y} = \boldsymbol{X}\boldsymbol{\beta} + \boldsymbol{\epsilon}. \tag{2}$$

with $\boldsymbol{y} = \left[\ln \tilde{S}(b_1, \boldsymbol{g}_1), ..., \ln \tilde{S}(b_N, \boldsymbol{g}_N)\right]^T$ and $\boldsymbol{X}$ is the design matrix of all diffusion gradient directions and strengths, which directly relates to the b-matrix (Mattiello et al., 1997). Furthermore, $\boldsymbol{\epsilon}$ denotes the column vector of independent error terms and $\boldsymbol{\beta}$ is the diffusion model's parameter vector, including all independent tensor elements and the noise-free non-DW signal. Obviously, N must be greater than or equal to the number of model parameters. Interestingly, Salvador et al. (2005) showed $\boldsymbol{\epsilon}$ to have expectation zero if the signal-to-noise ratio (SNR) of the DW images exceeds two (see appendix and Fig. 1(a)). Under that condition, the linear least squares (LLS) estimator of $\boldsymbol{\beta}$:

$$\hat{\boldsymbol{\beta}} = \left(\boldsymbol{X}^T\boldsymbol{X}\right)^{-1}\boldsymbol{X}^T\boldsymbol{y}, \tag{3}$$

is unbiased. However, (Salvador et al., 2005) also showed that the variance of $\boldsymbol{\epsilon}$ depends on the respective noise-free signals (see Fig. 1(b)):

$$Var(\boldsymbol{\epsilon}) = \left[\frac{\sigma^2}{S^2(b_1, \boldsymbol{g}_1)}, ..., \frac{\sigma^2}{S^2(b_N, \boldsymbol{g}_N)}\right], \tag{4}$$

with $\boldsymbol{S}(b, \boldsymbol{g}) = \{S(b_i, \boldsymbol{g}_i) : i = 1, ..., N\}$ the noise-free DW signals and σ the noise level. The best linear unbiased estimator (BLUE) of $\boldsymbol{\beta}$, i.e. the estimator with the highest precision within the class of unbiased linear estimators, can thus only be designed by including weights that equal the (scaled) reciprocal of the variance of the corresponding error terms (Eq. [4]):

$$\hat{\boldsymbol{\beta}} = \left(\boldsymbol{X}^T\boldsymbol{W}\boldsymbol{X}\right)^{-1}\boldsymbol{X}^T\boldsymbol{W}\boldsymbol{y}, \tag{5}$$

with

$$\boldsymbol{W} = \mathrm{diag}\left(\boldsymbol{S}^2(b, \boldsymbol{g})\right). \tag{6}$$

Obviously, the noise-free DW signals are not known and, as such, the weight matrix $\boldsymbol{W}$ needs to be estimated. Two suggested approaches are:

(a) WLLS_1: $\tilde{\boldsymbol{W}} = \mathrm{diag}\left(\tilde{\boldsymbol{S}}^2(b, \boldsymbol{g})\right)$, the weight are the squares of the respective noisy DW signals (Basser et al., 1994a; Koay et al., 2006);

(b) WLLS_2: $\tilde{\boldsymbol{W}} = \mathrm{diag}\left(\exp\left(2\boldsymbol{X}\hat{\boldsymbol{\beta}}_{\mathrm{LLS}}\right)\right)$, the weights are the preliminary estimates of $\boldsymbol{S}^2(b, \boldsymbol{g})$, reconstructed from the LLS estimate of $\boldsymbol{\beta}$ (Salvador et al., 2005).

The subindices of WLLS indicate that (a) and (b) are single-step and dual-step strategies, respectively. The estimation of $\boldsymbol{W}$ can iteratively be improved (Salvador et al., 2005). The weight matrix for the n^{th} iteration is given by the predicted DW signals from the previous estimate of the diffusion model parameters ($\hat{\boldsymbol{\beta}}_{n-1}$):

$$\tilde{\boldsymbol{W}}_n = \mathrm{diag}\left(\exp\left(2\boldsymbol{X}\hat{\boldsymbol{\beta}}_{n-1}\right)\right). \tag{7}$$

This iterative WLLS can be initialized by (a) or (b), which will be referred to as IWLLS_1 and IWLLS_2, respectively.

2.3. *Simulation experiments*

Monte Carlo simulations (50000 trials) were performed to evaluate the performance of the different strategies in the estimation of fractional anisotropy (FA), mean diffusivity (MD) and mean kurtosis (MK). In addition to the linear estimators described in section 2.2, the ordinary nonlinear least squares (NLS; (Koay et al., 2006)) estimator, initialized by a guess through WLLS_2, was evaluated. Throughout all experiments, FA and MD were estimated with the DTI model, whereas the MK was estimated with the DKI model.

2.3.1. *Simulation experiment 1*

The accuracy and the precision of the different estimators were evaluated as a function of the SNR of the Rician distributed signals. The SNR is here defined as the ratio between the non-DW signal and the noise level (cfr. Jones and Basser (2004)). For the DTI model, the MD and FA were set to $0.8 \times 10^{-3}\,\text{mm}^2/\text{s}$ and 0.85, respectively. The b-value was $1000\,\text{s}/\text{mm}^2$, and 60 gradient directions – isotropically distributed over a unit sphere using Coulomb's law of repulsion (Jones et al., 1999) – were used. We included five non-DW signals. For the DKI simulations, additional DW signals with $b = 2500\,\text{s}/\text{mm}^2$ were sampled along the same 60 directions. The MK was defined as 1.05, which is in agreement with values typically observed in the corpus callosum of the healthy human brain (Lätt et al., 2012). Noisy synthetic data were obtained by adding zero-mean complex Gaussian noise to the noise-free DW signals, which were calculated from the ground truth tensors using Eq. [1]. The absolute value of the resulting complex noisy signals was taken afterwards to obtain their magnitudes.

2.3.2. *Simulation experiment 2*

We evaluated the influence of the number of gradient directions per b-value shell on the accuracy of WLLS. Unlike the initial simulation experiment, the SNR was kept constant at the level of 20, whereas the number of gradient direction per shell varied from 6 to 120 for DTI and from 15 to 120 for DKI.

2.3.3. *Simulation experiment 3*

The effect of increasing the number of iterations (n) on the iterative WLLS approaches was evaluated. Now, the SNR was kept constant at the level of 20, whereas n varied from one to ten.

2.3.4. *Simulation experiment 4*

Rician distributed simulation data sets, representing the human white matter, were used for comparing the mean squared error (MSE) of each least squares method in estimating the diffusion parameters. The simulated data sets were constructed as follows. First, ground truth tensors were obtained by voxel-wise fitting the DKI model to a real data set (see section 2.4). Second, a set of noise-free DW signals was reconstructed from those diffusion tensors using the DTI and DKI model for the DTI and DKI analyses, respectively. Gradient directions and b-values were in agreement with the single-voxel experiments. Third, 5000 sets of noisy DW signals with an uniform SNR of 20 were generated by adding 5000 realizations of complex Gaussian noise to the noise-free DW signals. From each set, the diffusion tensors were estimated. From the 5000 estimates of FA, MD, and MK at each voxel for either of the estimators, the MSE was computed.

2.4. *Real data experiments*

Following DW data sets of healthy volunteers were acquired:

Data set 1: A first DW data set was collected on a 3T Philips Achieva MR scanner, using a 8-channel receiver head coil. Diffusion sensitizing was applied along 60 isotropically distributed gradient directions with $b = 1200\,\mathrm{s/mm^2}$ as well as $b = 2500\,\mathrm{s/mm^2}$. Additionally, one image without diffusion sensitization was acquired. Other imaging parameters were kept constant throughout the DW data acquisition sequences: TR/TE : 10265/107 ms; in-plan resolution: $1.75\times1.75\,\mathrm{mm^2}$; NEX: 1; slice thickness: 2 mm; axial slices: 70; and parallel imaging: SENSE with acceleration factor 2.

Data set 2: A second DW data set was acquired on a 1.5T Siemens MR system using a single receiver coil. A gradient configuration with 60 isotropically distributed gradient directions with $b = 700\,\mathrm{s/mm^2}$ was used. 10 non-DW images were additionally acquired. Other acquisition parameters were as follows: TR/TE : 8300/108 ms; in-plan resolution: $2\times2\,\mathrm{mm^2}$; NEX: 1; slice thickness: 2 mm; axial slices: 60.

Data set 3: A third DW data set was acquired on a Siemens Trio (3T) MR scanner, using a 12-channel receiver head coil. Diffusion weighting was applied along 60 isotropically distributed gradient directions with $b = 1000\,\mathrm{s/mm^2}$ as well as $b = 2500\,\mathrm{s/mm^2}$. Additionally, 10 non-DW imags were acquired. Other imaging parameters were kept constant: TR/TE : 6100/118 ms, in-plan resolution: $2.5\times2.5\,\mathrm{mm^2}$; NEX: 1; slice thickness: 2.5 mm; axial slices: 40; and parallel imaging factor: mSENSE with acceleration factor 2.

DW data were corrected for motion and eddy currents, including signal modulation and b-matrix rotation (Leemans et al., 2009; Leemans and Jones, 2009). Next, if the diffusion protocol met the minimal DKI requirements (Lu et al., 2006), a DKI analysis was performed in addition to a DTI analysis, during which all high b-valued – $b > 1500\,\mathrm{mm^2/s}$ – DW images were excluded. Since *data set 2* has only a single nonzero b-value shell, a DKI analysis was not possible. FA and MD maps were calculated from the DTI analysis, whereas the optional DKI analysis resulted in a MK map. The percentage differences in the estimation of the diffusion parameters of the different estimators, compared to a *bronze standard* were calculated. As a bronze standard, we adopted the previously proposed parameter estimation framework, consisting of the estimation of a (spatially varying) noise map and an accurate parameter estimator, i.e. the conditional least squares estimator, which properly accounts for the Rician distribution of all acquired DW data (Veraart et al., 2012; Dietrich et al., 2008).

3. Results

3.1. *Simulation experiments*

3.1.1. *Simulation experiment 1*

In Fig. 2, the estimates in FA, MD, and MK are compared among different estimators in terms of accuracy, precision, and MSE as a function of SNR^{-1}. The FA, MD, and MK values – calculated from the average model parameters – strongly vary across the different estimators (see Fig. 2(a-c)). Generally, the NLS estimator shows a large difference to the reference values, compared to the unweighted and weighted linear approaches. However, note that non-optimal weighting might reduce the accuracy of the estimator. The practical WLLS approaches, i.e. WLLS_1 and WLLS_2 show a lower accuracy than LLS and BLUE. Remarkably, the drop in accuracy is especially large for WLLS_1. While the accuracy of WLLS_2 is only slightly lower than BLUE, the WLLS_1 performs even worse than NLS in terms of accuracy. At very low SNR, e.g., due to the use of high b-values, all least squares estimators are inherently biased. In terms of precision (see Fig. 2(d-f)), all weighted linear estimators outperform the unweighted alternative. The LLS has low performance in terms of MSE because of the low precision, whereas the high MSE of WLLS_1 results from its low accuracy (see Fig. 2(g,h)). For the MSE in the estimation of MK (see Fig. 2(i)), the low accuracy of NLS and WLLS_1 is strongly counterbalanced by their high precision. Therefore, both estimators have a relatively low MSE. Simulations beyond these single-voxel experiments are needed to avoid overinterpretation of that observation (see section 3.1.4). In general, the differences between the estimators diminish with increasing SNR.

3.1.2. Simulation experiment 2

In Fig. 3, the influence of the number of gradient directions per b-value shell on the accuracy of the different estimators is shown. The accuracy of WLLS_2 increases steadily with increasing number of gradient directions due to the increasing precision of the LLS estimator or, as such, the increasing precision of the predicted DW signals. By contrast, with a low number of gradient directions, the difference between WLLS_1 and WLLS_2 in terms of accuracy vanishes due the reduced performance of WLLS_2. The combination of a low SNR of DW signals and a low precision of $\hat{\boldsymbol{\beta}}_{\text{LLS}}$, e.g., due to the limited number of DW samples, might result in outliers in the reconstructed DW signals, and thus, in the weight terms. Those outliers lower the accuracy of WLLS_2, compared to WLLS_1 and NLS (see e.g., Fig. 3(c)).

3.1.3. Simulation experiment 3

In Fig. 4, the effect of iterations on the performance of (I)WLLS estimators is shown. The graphs indicate that after a few iterations, both IWLLS estimators already closely approximate the performance of the BLUE, in terms of accuracy, precision, and MSE. The effect of the initial weighting matrix already vanishes for $n > 1$. Those findings are observed for all diffusion metrics.

3.1.4. Simulation experiment 4

In Fig. 5 and Fig. 6, scatter plots of the MSE in the estimation of FA, MD, and MK of all WLLS approaches against that of LLS and NLS, respectively, are shown. First, on average, the WLLS_1 has a significantly higher MSE in the estimation of MD and MK than LLS, WLLS_2, $\text{WLLS}_{1,2}$ ($n = 5$), and NLS. For FA, the WLLS_1 has a significantly higher MSE than WLLS_2, $\text{WLLS}_{1,2}$, and NLS. However, its MSE in the estimation of FA is significantly lower than the corresponding MSE of LLS. Second, the WLLS_2 has a significant lower MSE in the estimation of FA, MD, and MK, compared to all other linear alternatives, including the $\text{WLLS}_{1,2}$. The same conclusion does not apply when comparing the estimator to NLS. WLLS_2 has significantly lower MSE in the estimation of MD than NLS, while it has significantly higher MSE in the estimation of FA and MK. Statistical significance ($P < 0.01$) was always shown with a paired Wilcoxon signed rank test.

3.2. Real data experiments

In Fig. 7, Fig. 8, and Fig. 9, the percentage differences in the estimation of FA, MD, and MK of the different estimators, compared to the *bronze standard*, are shown for a single slice of each data set, respectively. The *bronze standard* maps are shown for anatomical reference (left column). The results are in-line with the simulation results. The WLLS_1 shows the largest differences compared to the reference maps. A large underestimation of both DTI indices and a large overestimation of MK can be observed. The same trends can be observed for all other estimators. The errors, however, are clearly more pronounced for the NLS estimator than for the LLS and the WLLS with well-chosen weights, i.e. WLLS_2 and both IWLLS estimators (only IWLLS_2 is shown). Unsurprisingly, the differences in the MK values are most prominent as the $b = 2500\,\mathrm{s/mm^2}$-shell has low SNR. The paired Wilcoxon signed rank test was applied to evaluate the pairwise differences between the estimated diffusion maps. All differences were statistically significant ($p < 0.01$).

4. Discussion

The DTI and DKI model have in common that they can be structured into a linear regression form depending on the natural logarithm of the DW MR signals. The unknown model parameters can be estimated with a LLS estimator, or its weighted variants. Those estimators are widely used in DTI and DKI studies, because they come with several strengths. First, the (weighted) LLS estimators have a closed-form solution. Therefore, unlike iterative nonlinear strategies, the linear estimators are computationally efficient and not prone to getting stuck in a local optimum. Second, the linear estimators are potentially very accurate, especially compared to the NLS estimator (Salvador et al., 2005). Under conditions that are discussed below, the linear estimators are even unbiased due to the null expectation of the error term in the log-Rician framework. Third, the high accuracy is not at the expense of the ease of use. In other words, unlike many advanced diffusion parameter estimators, e.g., the maximum likelihood (ML) estimator, the linear estimators don't require the knowledge of the noise parameter (Veraart et al., 2012). The estimation of the noise parameter is not only challenging, it also reduces the precision of the diffusion parameter estimator. Unfortunately, those advantages go hand in hand with some limitations and potential pitfalls. Some of them are to the best of our knowledge still unrecognized.

The unbiasedness of the linear estimators, even under inequality of variances, is subject to two conditions: the SNR of the DW signals should not be too low (> 2) and the DW data are assumed to be Rician distributed before the log-transformation. Those conditions might not be fulfilled because the use of high b-values or high spatial resolution, magnitude image operations prior to model fitting (Rohde et al., 2004; Veraart et al., 2012), or the use of parallel MR imaging techniques (Aja-Fernández et al., 2011; Aja-Fernández and Tristán-Vega, 2012). Indeed, our simulation and real data experiments confirmed that systematic errors in the calculation of quantitative parameters of clinical interest such as FA, MD, and MK will appear by lowering the SNR. The bias becomes even more prominent for multichannel and/or accelerated MRI reconstruction techniques that generate non-Rician distributed data (e.g., GRAPPA (Griswold et al., 2002) or homodyne partial fourier reconstruction (Noll et al., 1991)) (Tristán-Vega et al., 2012; Veraart et al., 2012). Furthermore, the accuracy of the linear estimators drops by applying operations such as motion correction and smoothing on the magnitude DW data as these might change the native data distribution (Veraart et al., 2012) . The mathematical reasoning of Salvador et al. (2005) then no longer holds. However, although motion and eddy current distortion correction was applied prior to tensor fitting in our real data study, the linear approaches still outperformed the NLS estimator in terms of accuracy.

The linearization of both diffusion models comes with the cost of a reduced precision of the diffusion parameter estimators. The cost, however, can be limited by accounting for the heteroscedasticity of the log-transformed data. The variances of the log-transformed Rician distributed magnitude MR signals must be known in order to design a WLLS estimator with optimal precision and accuracy. Unfortunately, the variances depend on the unknown noise-free DW signals (Salvador et al., 2005). Therefore, the best linear unbiased estimator (BLUE), i.e. the unbiased linear estimator with the highest precision, does not exist in practice. Nevertheless, we showed that optimal linear performance can be well approximated by a WLLS estimator for which the weight terms are estimated from noisy data with SNR>2. The approximation improves by drawing more DW samples or by iteratively updating the estimate of the weight matrix. In practice, only a few iterations are needed for convergence.

Already in the early days of DTI, (Basser et al., 1994a) stated that the weights for the WLLS can simply be the squares of the respective noisy DW signals (cfr. WLLS_1). More than a decade later, the statement was repeated by Koay et al. (2006). Many widely used software packages (e.g., ExploreDTI v4.8.2 (Leemans et al., 2009), FSL v5.0.1 (Jenkinson et al., 2012), Tortoise v1.3.1 (Pierpaoli et al., 2010)) and, as such, numerous researchers working the field of dMRI, adopted the approach. In the meantime, Salvador et al. (2005) proposed alternative, multi-step weighting schemes. In those approaches, the weights are the squares of the predicted signals, which are reconstructed from a previous estimate of the diffusion model parameters, obtained with the unweighted LLS estimator (cfr. WLLS_2) or a previous iteration of the WLLS estimator (cfr. IWLLS). The latter strategy was adopted by software packages such as Camino (Cook et al., 2006) and Slicer v4.2.1 (Pieper et al., 2006). So, nowadays, different weighting strategies are commonly used in a daily practice. This lack of unity not only obstructs multi-center research, it might also lead to misleading conclusions or irreproducible results. Indeed, we showed in this work that the performance of the WLLS strongly depends on the selected weight terms. More specifically, ill-chosen weights strongly reduce the accuracy of the linear estimator. Simulation and real data experiments indicated that the strategy proposed by Basser et al. (1994a) (WLLS_1) is the least favorable weighting strategy. Therefore, we suggest always opting for multi-step weighting strategies.

If the number of DW samples and the SNR are low, then the DW signals predicted from the LLS estimates, may contain outliers. A weight matrix including such outliers hampers the accuracy of the WLLS_2 estimator. Increasing the number of DW samples thus not only improves the precision of the WLLS_2 estimator, it also improves its accuracy. The latter does not hold for WLLS_1. Recently, it has been suggested to use non-linear tensor estimators rather than its linear alternatives (Jones et al., 2012). Our results, however, indicate the non-triviality in choosing between multi-step WLLS and NLS strategies for estimating dMRI parameters. Indeed, the decision depends on the number of DW signals (see Fig. 3), the parameter of interest (see Fig. 6), and – possibly – the actual data distribution. However, further study is needed to extensively showcase the strengths, limitations, and pitfalls of the different diffusion estimators in case of non-Rician data distributions.

5. Conclusion

Within the wealth of different diffusion parameter estimators, the WLLS estimator stands out by its simplicity and elegance. To date, no consensus has been reached on how to use the estimator in practice. In this work, it has been shown that the accuracy of the WLLS estimator strongly depends on the selected weight terms. A comparison of the most common weighting strategies indicated that the squares of the noisy DW signals should not be used if one is interested in designing a linear estimator with the highest achievable accuracy. However, if multi-step weighting strategies are applied, the weighted linear least squares estimator shows high performance characteristics in terms of accuracy/precision and may even be preferred over nonlinear estimation methods.

6. Acknowledgment

This work was supported by the Institute for the Promotion of Innovation through Science and Technology in Flanders (IWT-Vlaanderen) and by the Interuniversity Attraction Poles Program initiated by the Belgian Science Policy Office.

Appendix

The bias of the weighted linear least squares estimator, defined Eq. [5], is given by

$$\text{bias}\left(\hat{\boldsymbol{\beta}}\right) = \mathbb{E}\left[\hat{\boldsymbol{\beta}}\right] - \boldsymbol{\beta} = \mathbb{E}\left[\left(\boldsymbol{X}^T\boldsymbol{W}\boldsymbol{X}\right)^{-1}\boldsymbol{X}^T\boldsymbol{W}\boldsymbol{\epsilon}\right]. \tag{8}$$

Under the assumption of a deterministic design matrix ($\boldsymbol{X}$) and weight matrix ($\boldsymbol{W}$), the estimator will be unbiased if the error term (ϵ) has null expectation. Salvador et al. (2005) derived an analytical expression for the expectation value of the error term, given that the linearized diffusion model is fitted to the natural logarithm of Rice distributed diffusion-weighted measurements ($\tilde{\boldsymbol{S}}$). The probability distribution function (PDF) of an arbitrary Rice distributed variable m is given by Sijbers et al. (1998):

$$f_m\left(m|m_0,\sigma\right) = \frac{m}{\sigma^2}\exp\left(-\frac{m^2+m_0^2}{2\sigma^2}\right) I_0\left(\frac{m\,m_0}{\sigma^2}\right), \tag{9}$$

with m_0 the noise-free signal, σ^2 the noise variance, and I_0 the zeroth order modified Bessel function of the first kind. The PDF of the log-transformed variable $m' = \ln(m)$ can be determined by substituting m in Eq. [9] by m':

$$\begin{aligned} f_{m'}\left(m'|m_0,\sigma\right) &= f_m\left(\exp(m')|m_0,\sigma\right)\frac{d\exp(m')}{dm'} \\ &= \frac{e^{2m'}}{\sigma^2}\exp\left(-\frac{e^{2m'}+m_0^2}{2\sigma^2}\right) I_0\left(\frac{e^{m'}\,m_0}{\sigma^2}\right). \end{aligned} \tag{10}$$

The expectation value of m' is given by:

$$\begin{aligned}\mathbb{E}\left[m'\right] &= \int\limits_{-\infty}^{\infty} m' f_{m'}\left(m'|m_0,\sigma\right) d\,m' \\ &= \int\limits_{\mathrm{SNR}^2/2}^{\infty} \frac{1}{t\,e^t} dt + \ln(m_0),\end{aligned} \tag{11}$$

with $\mathrm{SNR} = \frac{m_0}{\sigma}$. If the error term ϵ is defined as $m' - \ln(m_0)$, then its expectation value can immediately be derived:

$$\begin{aligned}\mathbb{E}\left[\epsilon\right] &= \mathbb{E}\left[m' - \ln(m_0)\right] \\ &= \int\limits_{\mathrm{SNR}^2/2}^{\infty} \frac{1}{t\,e^t} dt + \ln(m_0) - \ln(m_0) \\ &= \int\limits_{\mathrm{SNR}^2/2}^{\infty} \frac{1}{t\,e^t} dt.\end{aligned} \tag{12}$$

In Fig. 1(a), $\mathbb{E}\left[\epsilon\right]$ is shown for different SNR values. It can be seen that for SNR > 2, the error terms is zero-centered. The potentially high accuracy of the (weighted) linear least squares estimators originates in this observation.

References

Aja-Fernández, S., Tristán-Vega, A., 2012. Influence of noise correlation in multiple-coil statistical models with sum of squares reconstruction. Magn Reson Med 67 (2), 580–585.

Aja-Fernández, S., Tristán-Vega, A., Hoge, W. S., 2011. Statistical noise analysis in GRAPPA using a parametrized noncentral chi approximation model. Magn Reson Med 65 (4), 1195–1206.

Andersson, J., 2008. Maximum a posteriori estimation of diffusion tensor parameters using a Rician noise model: Why, how and but? NeuroImage 42 (4), 1340–1356.

Basser, P. J., Mattiello, J., Le Bihan, D., March 1994a. Estimation of the effective self-diffusion tensor from the NMR spin echo. J Magn Reson B 103 (3), 247–254.

Basser, P. J., Mattiello, J., Le Bihan, D., January 1994b. MR diffusion tensor spectroscopy and imaging. Biophys J 66 (1), 259–267.

Bihan, D. L., Johansen-Berg, H., 2012. Diffusion MRI at 25: Exploring brain tissue structure and function. NeuroImage 61 (2), 324–341.

Cook, P. A., Bai, Y., Nedjati-Gilani, S., Seunarine, K. K., Hall, M. G., Parker, G. J., Alexander, D. C., 2006. Camino: Open-Source Diffusion-MRI Reconstruction and Processing. In: Proceedings 14th Scientific Meeting of the International Society for Magnetic Resonance in Medicine. Seattle, USA, p. 2759.

Dietrich, O., Raya, J. G., Reeder, S. B., Ingrisch, M., Reiser, M. F., Schoenberg, S. O., 2008. Influence of multichannel combination, parallel imaging and other reconstruction techniques on MRI noise characteristics. Magn Reson Imaging 26 (6), 754–762.

Griswold, M. A., Jakob, P. M., Heidemann, R. M., Nittka, M., Jellus, V., Wang, J., Kiefer, B., Haase, A., 2002. Generalized autocalibrating partially parallel acquisitions (GRAPPA). Magn Reson Med 47 (6), 1202–1210.

Jenkinson, M., Beckmann, C. F., Behrens, T. E., Woolrich, M. W., Smith, S. M., 2012. FSL. NeuroImage 62 (2), 782 – 790.

Jensen, J. H., Helpern, J. A., Ramani, A., Lu, H., Kaczynski, K., Jun. 2005. Diffusional kurtosis imaging: the quantification of non-gaussian water diffusion by means of magnetic resonance imaging. Magn Reson Med 53 (6), 1432–40.

Jones, D. K., Basser, P. J., 2004. Squashing peanuts and smashing pumpkins: How noise distorts diffusion-weighted MR data. Magn Reson Med 52 (5), 979–993.

Jones, D. K., Horsfield, M. A., Simmons, A., 1999. Optimal strategies for measuring diffusion in anisotropic systems by magnetic resonance imaging. Magn Reson Med 42 (3), 515–525.

Jones, D. K., Knösche, T. R., Turner, R., 2012. White matter integrity, fiber count, and other fallacies: The do's and don'ts of diffusion MRI. NeuroImage (0), doi: 10.1016/j.neuroimage.2012.06.081.

Kiselev, V. G., 2010. The cumulant expansion: an overarching mathematical framework for understanding diffusion NMR. In: Diffusion MRI: theory, methods, and apllications. Oxford University Press: Oxford, pp. 152–168.

Koay, C. G., Chang, L. C., Carew, J. D., Pierpaoli, C., Basser, P. J., 2006. A unifying theoretical and algorithmic framework for least squares methods of estimation in diffusion tensor imaging. J Magn Reson 182 (1), 115–125.

Koay, C. G., Ozarslan, E., Basser, P. J., 2009. A signal transformational framework for breaking the noise floor and its applications in MRI. J Magn Reson Imaging 197 (2), 108 – 119.

Kristoffersen, A., Aug. 2007. Optimal estimation of the diffusion coefficient from non-averaged and averaged noisy magnitude data. J Magn Reson Imaging 187 (2), 293–305.

Kristoffersen, A., Oct. 2011. Estimating non-Gaussian diffusion model parameters in the presence of physiological noise and Rician signal bias. J Magn Reson Imaging, 1–9.

Landman, B., Bazin, P.-L., Prince, J., oct. 2007. Diffusion tensor estimation by maximizing Rician likelihood. In: IEEE 11th International Conference on Computer Vision, 2007. Rio de Janeiro, Brazil, pp. 1 –8.

Lätt, J., Nilsson, M., Wirestam, R., Stahlberg, F., Karlsson, N., Johansson, M., Sundgren, P. C., van Westen, D., 2012. Regional values of diffusional kurtosis estimates in the healthy brain. J Magn Reson Imaging, doi: 10.1002/jmri.23857.

Leemans, A., Jeurissen, B., Sijbers, J., Jones, D. K., 2009. ExploreDTI: a graphical toolbox for processing, analyzing, and visualizing diffusion MR data. In: Proceedings 17th Scientific Meeting, International Society for Magnetic Resonance in Medicine. Honolulu, USA, p. 3537.

Leemans, A., Jones, D. K., 2009. The B-matrix must be rotated when correcting for subject motion in DTI data. Magn Reson Med 61 (6), 1336–1349.

Lu, H., Jensen, J. H., Ramani, A., Helpern, J. A., 2006. Three-dimensional characterization of non-Gaussian water diffusion in humans using diffusion kurtosis imaging. NMR Biomed 19 (2), 236–247.
URL http://www.ncbi.nlm.nih.gov/pubmed/16521095

Mattiello, J., Basser, P., Le Bihan, D., 1997. The b-matrix in diffusion tensor echo-planar imaging. Magn Reson Med 37 (2), 292–300.

Noll, D., Nishimura, D., Macovski, A., jun 1991. Homodyne detection in magnetic resonance imaging. IEEE Transactions on Medical Imaging 10 (2), 154 –163.

Pieper, S., Lorensen, B., Schroeder, W., Kikinis, R., 2006. The NA-MIC Kit: ITK, VTK, Pipelines, Grids and 3D Slicer as an Open Platform for the Medical Image Computing Community. In: Proceedings of the 3rd IEEE International Symposium on Biomedical Imaging: From Nano to Macro. Arlington, USA, pp. 698–701.

Pierpaoli, C., Walker, L., Irfanoglu, M., Barnett, A., Basser, P., Chang, L., Koay, C., Pajevic, S., Rohde, G., Sarlls, J., Wu, M., 2010. TORTOISE: an integrated software package for processing of diffusion MRI data. In: Proceedings 18th Scientific Meeting, International Society for Magnetic Resonance in Medicine. Stockholm, Sweden, p. 1597.

Rohde, G., Barnett, A., Basser, P., Marenco, S., Pierpaoli, C., 2004. Comprehensive approach for correction of motion and distortion in diffusion-weighted MRI. Magn Reson Med 51 (1), 103–114.

Salvador, R., Peña, A., Menon, D. K., Carpenter, T. A., Pickard, J. D., Bullmore, E. T., 2005. Formal characterization and extension of the linearized diffusion tensor model. Human Brain Mapping 24 (2), 144–155.

Sijbers, J., den Dekker, A. J., Scheunders, P., Van Dyck, D., June 1998. Maximum likelihood estimation of Rician distribution parameters. IEEE Transactions on Medical Imaging 17 (3), 357–361.

Tristán-Vega, A., Aja-Fernández, S., Westin, C., 2012. Least squares for diffusion tensor estimation revisited: Propagation of uncertainty with Rician and non-Rician signals. NeuroImage 59 (4), 4032–4043.

Veraart, J., Rajan, J., Peeters, R., Leemans, A., Sunaert, S., Sijbers, J., 2012. A comprehensive framework for accurate diffusion MRI parameter estimation. Magn Reson Med, doi: 10.1002/mrm.24529.

Veraart, J., Van Hecke, W., Sijbers, J., 2011. Constrained maximum likelihood estimation of the diffusion kurtosis tensor using a Rician noise model. Magn Reson Med 66 (3), 678–686.

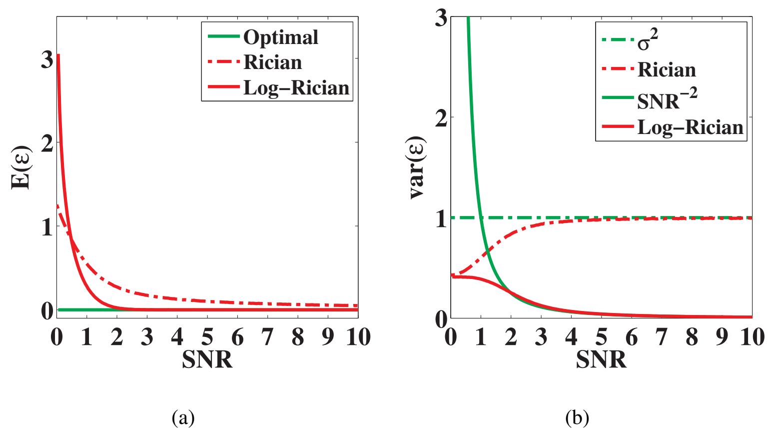

Figure 1: The expectation value (a) and variance (b) of the error term before and after linearizion by taking the natural logarithm of the Rice distributed variables is shown as a function of the SNR. In the log-Rician framework the residuals have null expectation if SNR > 2. The variance, on the other hand, is then well-approximated by SNR^{-2}. Both curves indicate the potentially high accuracy and precision of WLLS. In the Rician framework, the slow convergence to null expectation reduces the accuracy of the NLS estimator.

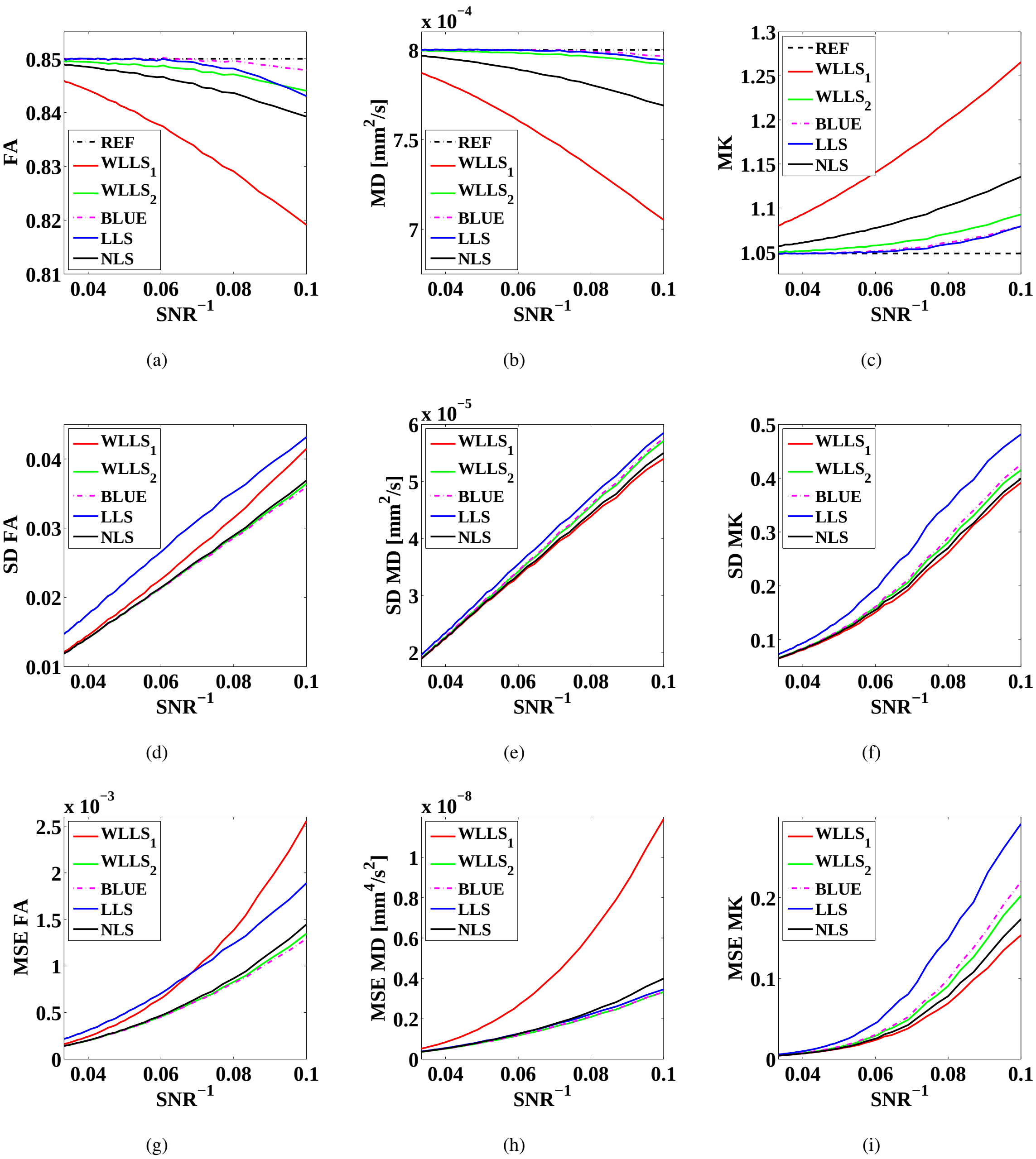

Figure 2: Simulation experiment 1: FA, MD, and MK calculated from the average model parameters (a-c), the standard deviation (SD) of the estimated diffusion parameters (d-f), and MSE in the estimation of FA, MD, and MK (g-i) are shown as a function of the SNR^{-1} for the different least squares estimators.

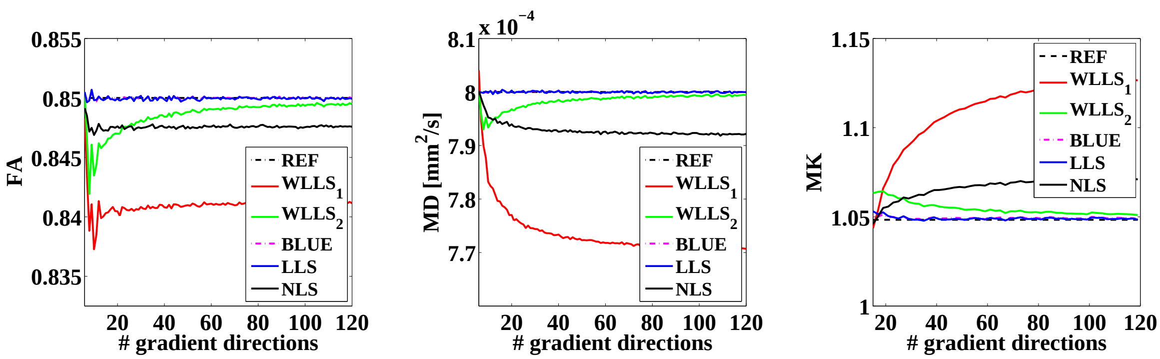

(a) (b) (c)

Figure 3: Simulation experiment 2: FA, MD, and MK calculated from the averaged model parameters are shown as a function of the number of gradient directions per b-value shell for the different least squares estimators.

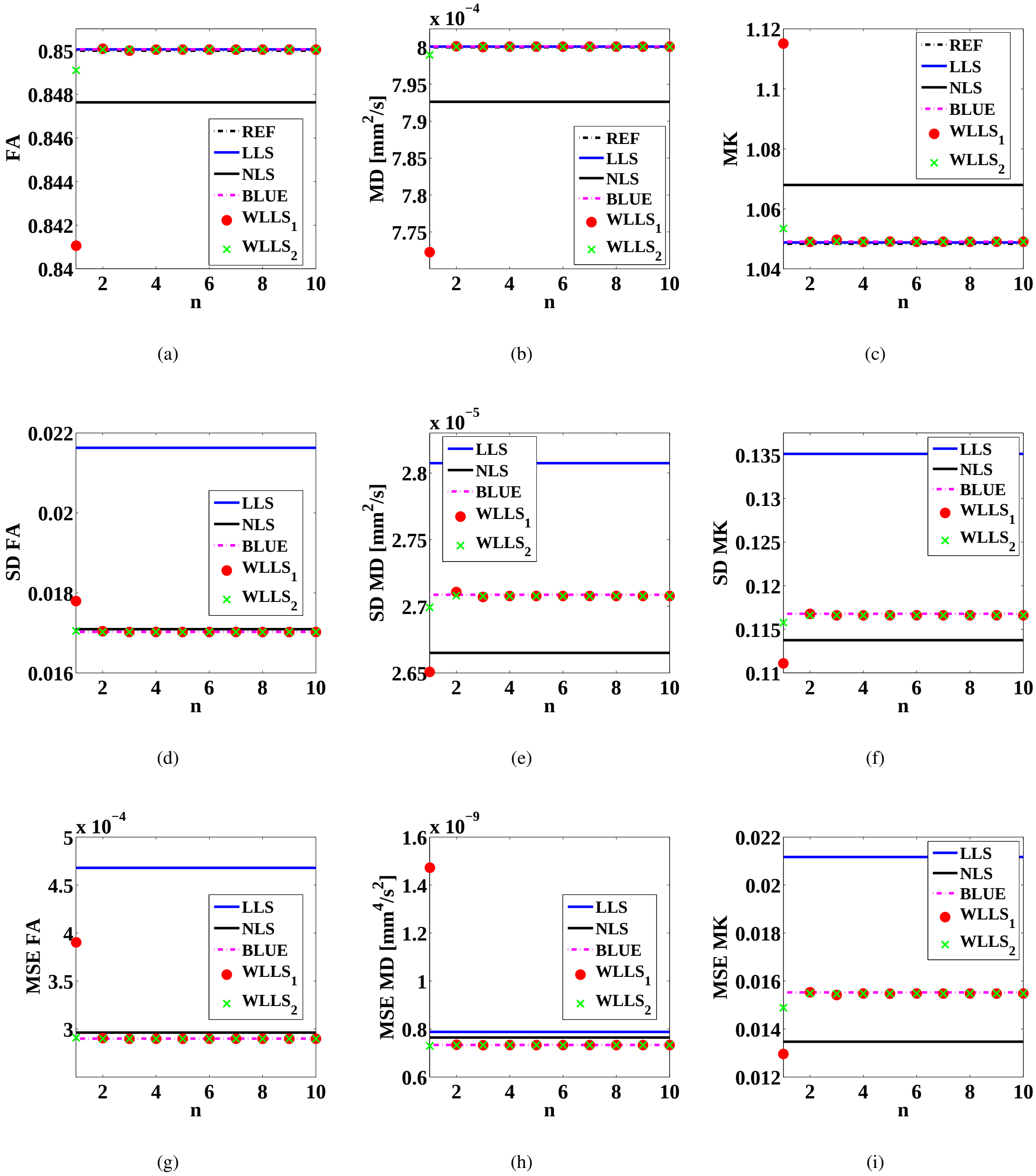

Figure 4: Simulation experiment 3: FA, MD, and MK calculated from the average model parameters (a-c), the standard deviation of the estimated diffusion parameters (d-f), and MSE in the estimation of FA, MD, and MK (g-i) are shown as a function of the number of iterations (n) for the different least squares estimators.

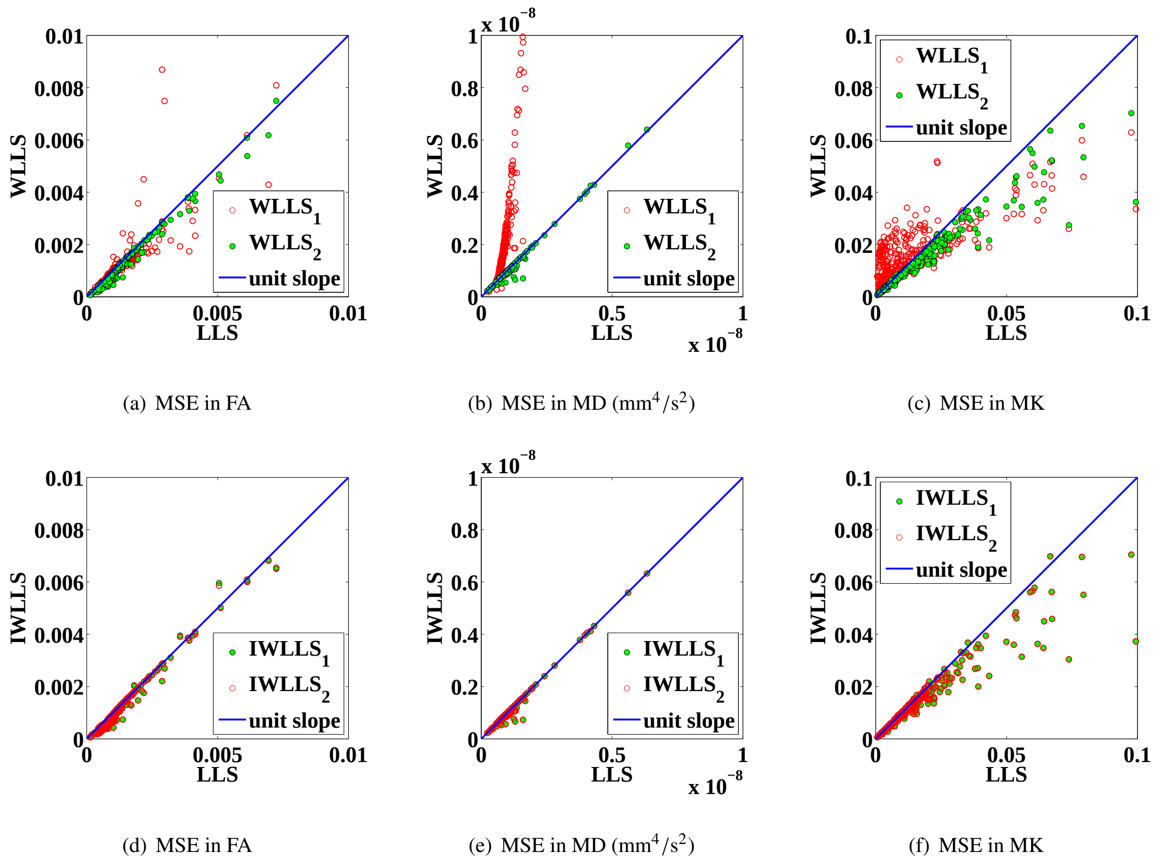

(a) MSE in FA

(b) MSE in MD (mm^4/s^2)

(c) MSE in MK

(d) MSE in FA

(e) MSE in MD (mm^4/s^2)

(f) MSE in MK

Figure 5: Simulation experiment 4: Scatter plots of the MSE of WLLS vs. LLS (a-c) and IWLLS vs. LLS (d-f) in estimating FA, MD, and MK. *red circles:* Initial weights of the WLLS approaches are the squares of the respective noisy DW signals – *green dots:* Initial weights are the predicted signal from an estimate of the diffusion model parameters, obtained with the unweighted LLS estimator. The blue lines are unit-slope-lines.

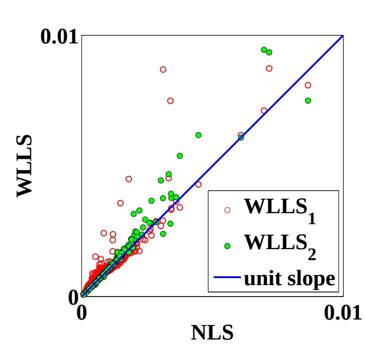

(a) MSE in FA

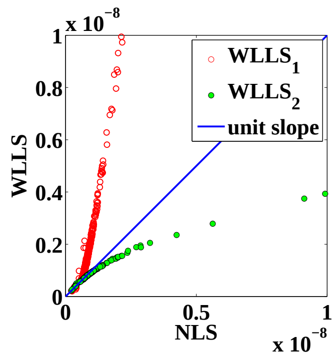

(b) MSE in MD (mm^4/s^2)

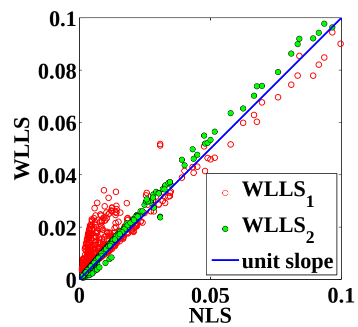

(c) MSE in MK

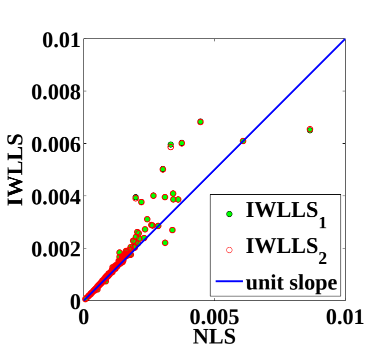

(d) MSE in FA

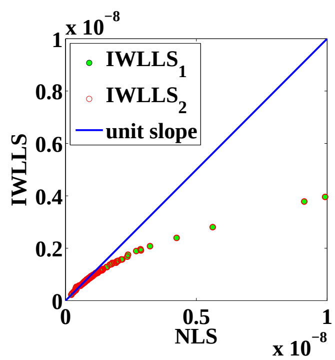

(e) MSE in MD (mm^4/s^2)

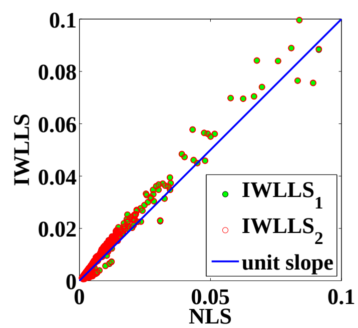

(f) MSE in MK

Figure 6: Simulation experiment 4: Scatter plots of the MSE of WLLS vs. NLS (a-c) and IWLLS vs. NLS (d-f) in estimating FA, MD, and MK. Color encoding cfr.Fig. 5

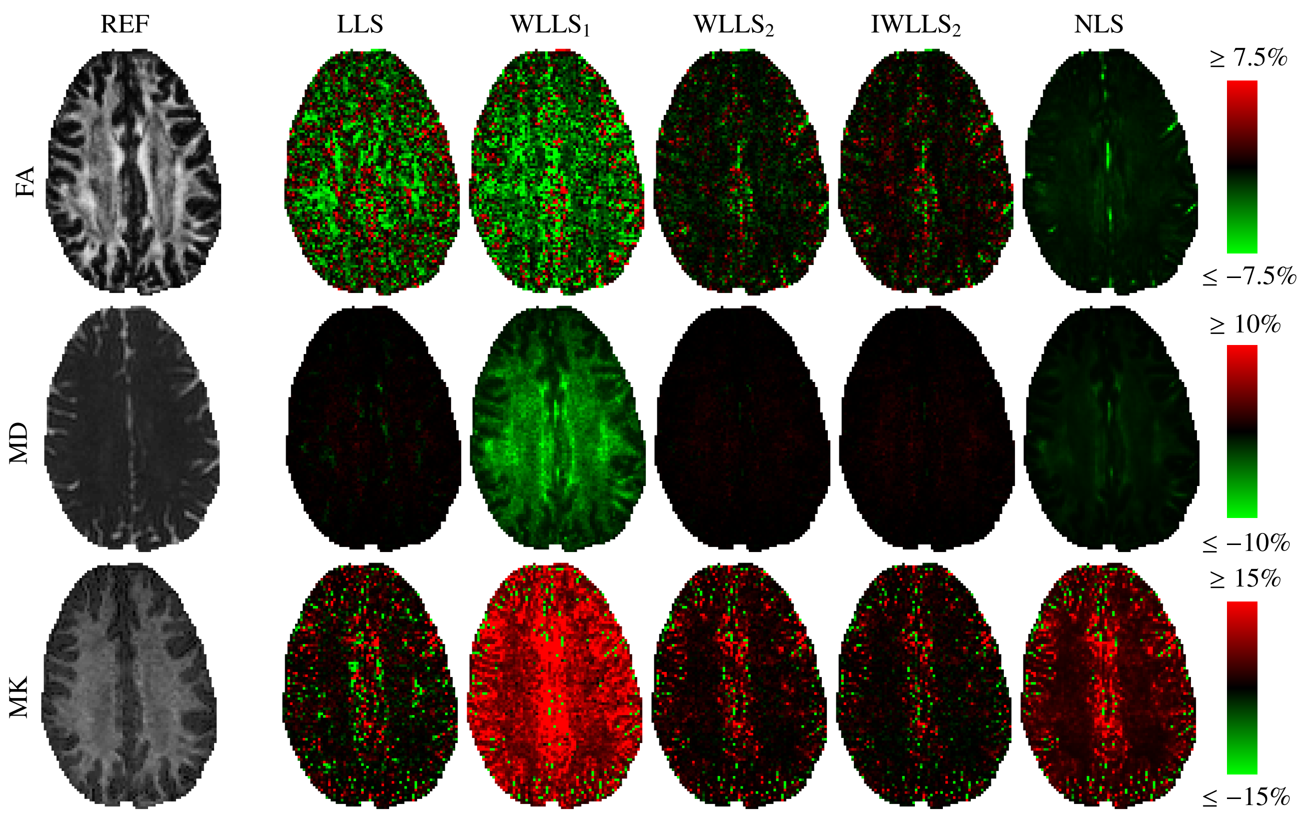

Figure 7: Real data set 1: The percentage differences between the FA, MD, and MK estimates for the least squares estimators and the bronze standard, i.e. an accurate diffusion parameter estimation framework, which accounts for the Rician data statistics. The bronze standard diffusion parameter maps are shown for anatomical reference (left column)

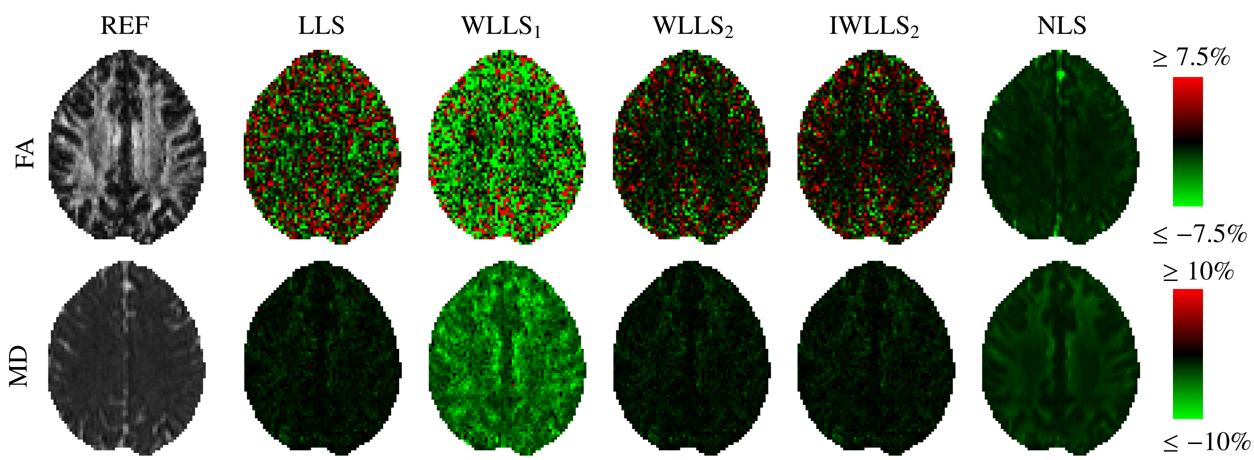

Figure 8: Real data set 2: The percentage differences between the FA, MD, and MK estimates for the least squares estimators and the bronze standard.

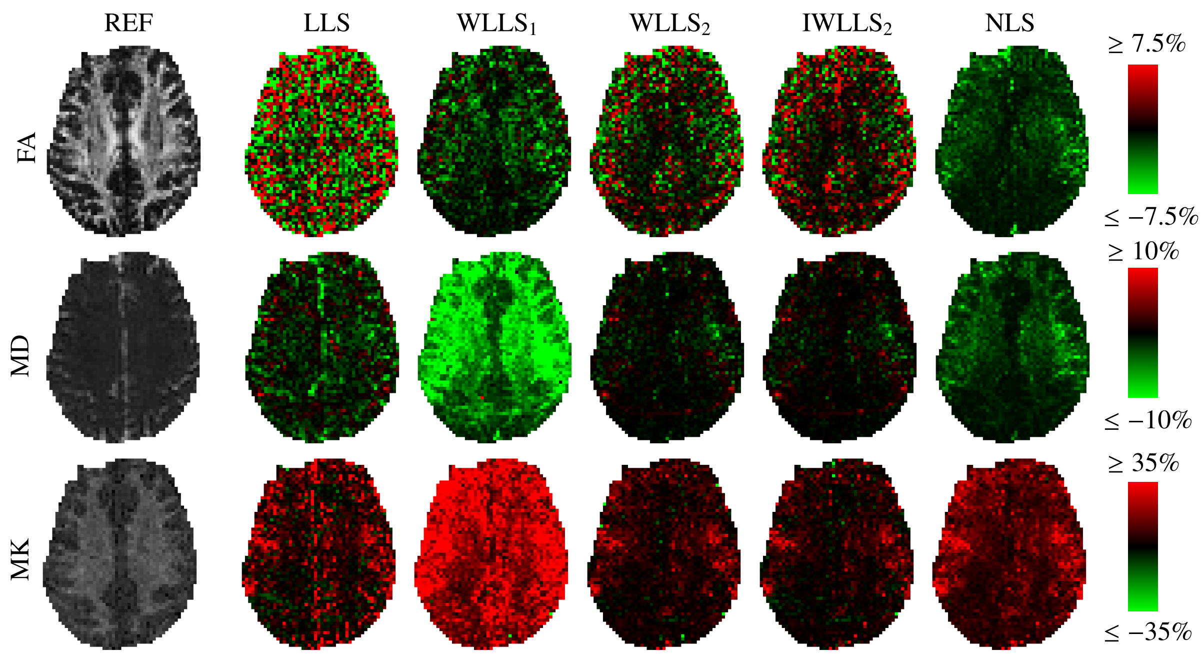

Figure 9: Real data set 3: The percentage differences between the FA, MD, and MK estimates for the least squares estimators and the bronze standard.